Int J Clin Exp Med 2016;9(6):10627-10638
www.ijcem.com /ISSN:1940-5901/IJCEM0020521

Original Article

Comparison of the properties of a native articular cartilage extracellular matrix-derived oriented scaffold and the chondro-gide bilayered scaffold-cartilage tissue engineering

Zimin Wang[1*], Jingliang Wang[2*], Huichao Wang[3*], Jingxiang Huang[1], Shuyun Liu[1], Yun Zhu[1], Yu Wang[1], Jiang Peng[1], Aiyuan Wang[1], Changlong Yu[1], Quanyi Guo[1], Peilan Wang[4]

[1]Key Laboratory of People's Liberation Army, Institute of Orthopedics, PLA General Hospital, Haidian, Beijing, China; [2]Department of Surgery, Second People Hospital of Koral Sinkiang Xinjiang, China; [3]Luoyang Orthopedic Hospital of Henan Province, Orthopedic Institute of Henna Province, Luoyang, Henan, China; [4]Out-patient Department, PLA General Hospital, 28 Fu-xing Road, Haidian, Beijing 100853, China. [*]Equal contributors.

Received November 25, 2015; Accepted April 14, 2016; Epub June 15, 2016; Published June 30, 2016

Abstract: Purpose: The objects of this study were to compare biological properties of a native articular cartilage extracellular matrix (ACECM)-derived oriented scaffold and the Chondro-Gide bilayered scaffold. Methods: The ACECM oriented scaffold (No. 4131) and the Chondro-Gide scaffold (No. 4132) compared form (I) The physical properties (II) FDA/PI staining, and frozen sections were stained with toluidine blue, safranin O, and alcian blue, as well as immunohistochemical staining for collagen types I and II. (III) Quantitative analyses (hydroxyproline content, determining the glycosaminoglycan (GAG) and DNA contents), and the expression of col I, col II, col X, aggrecan, and SOX-9 via RT-PCR. (IV) The two scaffolds were implanted subcutaneously in rats. Results: The two scaffolds have different characteristics in diameters, porosity, water absorption expansion coefficient, biomechanical compression stiffness, elastic modulus, FDA/PI staining, toluidine blue, safranin O, alcian blue, type II collagen, type I collagen. The MTT toxicity of the scaffolds was Grade I and Grade II respectively. The adhesion rates were different in two scaffolds. The content of hydroxyproline, GAG, DNA and gene expression (Col I, Col II, aggrecan, Sox-9, and Col X) was calculated in 4131 and 4132. After subcutaneous implantation in rats, the sections were pathologically graded as 'qualified'. Conclusions: The two scaffolds have different characteristics.

Keywords: Cartilage tissue engineering, scaffold, cartilage biomaterials, comparison of properties

Introduction

Articular cartilage tissue engineering [1-3] is a rapidly developing field aimed at regenerating articular cartilage. Although certain cartilage tissue engineering techniques have been used clinically, addressing several issues in articular cartilage repair, the repaired tissues do not completely recover the normal hyaline cartilage structure and function. Therefore, further studies are needed. In the present study, a novel oriented scaffold made from decellularized cartilage extracellular matrix is described, and its properties are compared to those of the commercially available Chondro-Gide cartilage scaffold that has been used clinically. The scaffolds were assessed in vitro to determine what advantages this biomimetic scaffold may have in clinical application.

Materials and methods

Scaffolds and instruments

The articular cartilage extracellular matrix (ACECM)-derived oriented scaffold (No. 4131) was prepared by the Orthopaedic Institute of the PLA General Hospital. The Chondro-Gide scaffold (No. 4132), which has been used in surgeries to repair articular cartilage defects in many cases, was purchased from a vendor.

The main instruments used were a light microscope (LM, Olympus, Tokyo, Japan), a scanning electron microscope (SEM; s-520, Hitachi, Ltd., Tokyo, Japan), a vacuum freeze-drying machine (Biocool Laboratory Instrument Co., Ltd., Beijing, China), a Bio-Link ultraviolet cross-linker, a biomechanical tester (ElectroForce 3100, Bose

Corporation, Framingham, MA, USA), and a low temperature ultra-speed centrifuge (Beckman Coulter, Brea, CA, USA).

Preparation of the ACECM oriented scaffolds (No. 4131)

Porcine articular cartilage blocks were ground down with the wet method. After differential centrifugation, the decellularized cartilage extracellular matrix components were collected. The ACECM-derived oriented scaffolds were prepared by the application of directional crystallization and freeze-drying technology, followed by physical and chemical cross-linking and sterilization with Co-60 γ-rays for future use.

Assessment of the physical properties of the scaffolds

Surface characteristics and porous channel structure: An 8-mm diameter 4131 ACECM oriented scaffold was cut into longitudinal and transverse sections with a thickness of 1 mm, and Chondro-Gide 4132 scaffolds were prepared with the same surface area. The surface shape and longitudinal and transverse pore structures of the two scaffolds were observed using dark field light microscopy. Sections of the two scaffolds were also prepared for scanning electron microscopy (SEM) by spray-coating the surface of the scaffolds with platinum. The longitudinal and transverse pore structures at the surfaces were observed by SEM.

Porosity

To measure the porosity, absolute ethanol was added to a graduated test tube to an initial volume V1. Six samples of each scaffold were cut into pieces of equal size, immersed in the tube for 5 min, degased with negative pressure to fill the scaffold pores with ethanol until no foam was emitted, and the final volume of ethanol with immersed scaffolds was recorded as V2. The scaffolds filled with ethanol were removed and the volume was recorded as V3. The porosity E of the scaffolds was calculated as E = (V1-V3)/(V2-V3). Each sample was tested three times and the mean values were used.

Water absorption expansion coefficient: The oriented scaffolds were cut into 6 1-cm-long pieces, soaked in deionized water for 10 min at room temperature, suspended over a sink for 1 min until no more water dribbled out, and weighed (wet weight, m). Next, the scaffolds were dried inside a vacuum drying oven for 12 h at 50°C and then weighed (dry weight, m_0). The water absorption rate X was calculated as $X = (m-m_0)/m$. Each sample was tested three times and the mean values were used.

Mechanical properties: A trephine with a diameter of 8 mm was used to drill 6 round test pieces at a height of 2 mm from each of the two scaffold types. These samples were placed on a biomechanical tester (ElectroForce 3100) to perform indentation testing to measure the elastic modulus and compression stiffness. The imposed pressure and deformation measured were used to plot the compressive stress - strain curve. The tangent slope in the linear region of the stress-strain curve was defined as the elastic modulus.

Qualitative analysis of rabbit cartilage cells seeded on the scaffolds

Cell viability: First, 6 mL of cartilage culture medium containing 15% fetal calf serum was added to 3rd generation rabbit cartilage cells. Next, the cells were seeded onto the front and back surfaces of the two types of 8-mm diameter, 2-mm thick scaffolds. The scaffolds were incubated at 37°C in a 5% CO_2 environment for 3 days, removed, stained with FDA/PI for viable cells, and observed with fluorescence microscopy.

Staining and immunohistochemistry: As above, 3rd generation rabbit cartilage cells were seeded onto the front and back surfaces of the two types of scaffolds. Each scaffold group had 6 wells in a single plate. Half a million cells were seeded into each well of the plate, and then 6 mL of cartilage culture media was added. The scaffolds were incubated at 37°C in a 5% CO_2 environment for 6 days, and then frozen sections were prepared and stained with toluidine blue (TO), safranin O, and alcian blue (AB). Immunohistochemical staining was performed with mouse anti-human types I and II collagen antibodies. The sections were observed under light microscopy.

Quantitative analysis of rabbit cartilage cells seed on the scaffolds

Cell toxicity of the scaffold: DMEM culture media was added to the two types of scaffolds based on surface area at 125 mm^2/mL, with 20 mL of the leaching liquid added to each

Table 1. Primer sequences of target genes used for RT-qPCR

Target genes	Primer sequence
Rbt gapdh	F: 5'-CAAGAAGGTGGTGAAGCAGG-3' R: 5'-CACTGTTGAAGTCGCAGGAG-3'
Rbt col1a2	F: 5'-GCCACCTGCCAGTCTTTACA-3' R: 5'-CCATCATCACCATCTCTGCCT-3'
Rbt col2a1	F: 5'-CACGCTCAAGTCCCTCAACA-3' R: 5'-TCTATCCAGTAGTCACCGCTCT-3'
Rbt sox-9	F: 5'-GCGGAGGAAGTCGGTGAAGAAT-3' R: 5'-AAGATGGCGTTGGGCGAGAT-3'
Rbt col10a1	F: 5'-CCACCAGGACAAGCAGTCAT-3' R: 5'-CACTAACAAGAGGCATCCCG-3'
Rbt aggrecan	F: 5'-GGAGGAGCAGGAGTTTGTCAA-3' R: 5'-TGTCCATCCGACCAGCGAAA-3'

group. The samples were placed at 37°C for 24 hours to allow leaching, and then fetal calf serum was added to 10%. L929 cells were seeded at 4,000 cells per 0.3 mL per well in 96-well plates. Three wells were seeded in each group for each analysis day. Fresh DMEM culture solution conditioned with L929 cells was used as the negative control. The cells were cultured in the leaching liquid at 37°C in a 5% CO_2 incubator for 1, 3, 5, or 7 days. One plate was tested each day, and a total of 4 tests were performed. For the test, 20 μL of MTT solution was added to each well. After 4 hours, the optical density (OD) of the well was read at 492 nm and the results were recorded for each group on each day.

Cell adhesion: To compare the adhesion of cells on the scaffolds, 3rd generation rabbit cartilage cells were seeded onto the two types of scaffolds with the same amount of surface area. Six wells were used in each group, and readings were taken at 3 and 6 hours 6, with 3 wells used for each time point and one scaffold specimen per well. Half a million cells were seeded onto each scaffold specimen within its well, 6 mL of cartilage culture media was added, and the plates were incubated at 37°C in a 5% $C0_2$ environment. The non-adherent cell suspensions in each well were aspirated and the number of cells counted using a hemocytometer to determine the % adhesion for the two types of scaffolds as adhesion % = count of adherent cells/total number of cells × 100%.

Total collagen content

The collagen content was normalized to the surface area of the scaffolds. Specimens of the two types of scaffolds were lysed using an alkaline lysis kit to allow the oxidative products of the hydroxyproline in the collagen, as oxidants, to interact with the dimethylaminobenzaldehyde to create a violet red color. The OD values of the samples were measured using a spectrophotometer, and then the content of hydroxyproline was calculated.

DNA content: Physical and physiochemical methods were used to prepare the scaffold samples (n = 3). First, the ECM was dissolved in sodium citrate, centrifuged at 2,000 r/min for 10 min, and the supernatant was removed. Next, edathamil and caroid were added to the samples in a 65°C water bath for 72 hours for lysis. The samples were centrifuged at 10,000 r/min for 5 min, and the supernatant was collected. The same amount of Hoechst33258 was added to the supernatants and to DNA extracted from calf thymus as standards, and fluorometric quantitative testing was performed to determine the DNA content in the samples.

Glycosaminoglycan (GAG) content: The chondroitin sulfate GAG content was measured with the employment of the positively charged dye dimethyl methylene blue (DMB) to generate color (the DMB method), which was quantified with UV spectrophotometry. Standard curves were created by adding 100 μL containing 10, 20, 40, 60, and 80 μg of chondroitin sulfate and 100 μL of deionized water as the blank control. Three mL of dimethyl methylene blue was added to each tube, equal portions were placed into quartz tubes, and UV spectrophotometry at 480 nm was used to assess the OD values and plot a standard curve. The scaffold samples were lyophilized, accurately weighed within about 1 mg, and caroid lysate was added for lysis at 65°C for 48 hours. The samples were then centrifuged at 1,500 r/min for 5 min, 100 μL of the lysate was removed, 3 mL of DMB was added, and the OD values at 480 nm were detected with UV spectrophotometry to calculate the content of GAG per unit weight of the scaffold after comparison with the standard curve.

RT-PCR analysis: Three 10-mm specimens of each of the two types of scaffolds were placed into the wells of 6-well plates for culture. Rabbit cartilage cells were added at 600,000 cells per well in 6 mL of culture media, and the media was changed once every 3 days. The samples

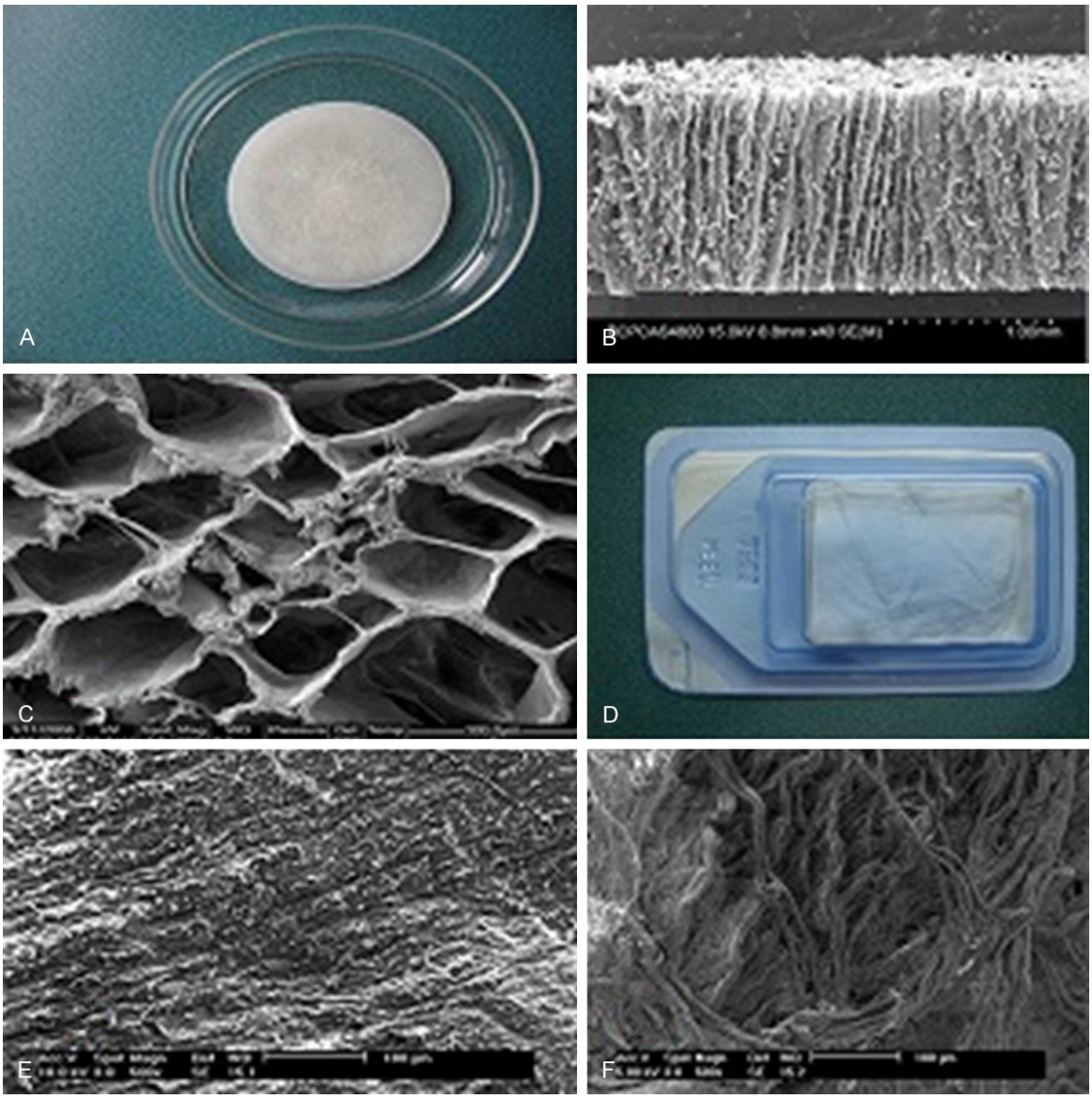

Figure 1. A: ACECM oriented scaffolds were generally round, white, spongy. B: ACECM oriented scaffolds was found by SEM. C: ACECM oriented scaffolds was found by SEM. D: Chondro-Gide scaffolds were white, generally square. E: The collagen of Chondro-Gide on the superficial layer was dense. F: The collagen of Chondro-Gide on the superficial layer was loose.

were cultured for 7 days at 37°C in a 5% CO_2 environment, and then the samples were harvested and cut into small pieces. TRIzol was added for lysis and extraction of total RNA for analysis. Five different primers were selected (**Table 1**), and RT-PCR cycle amplification was performed to determine the expression levels of the 5 genes.

Subcutaneous implantation of the scaffolds in rats

After the two scaffolds were implanted subcutaneously in rats, pathological grading was performed. The scaffold materials were harvested from the rats after euthanasia at weeks 1, 2, and 4 after implantation. Paraffin sections were prepared, stained with HE, observed under light microscopy, and graded based on the number of inflammatory cells, lymphocytes, and the thickness of the cyst wall formed around the tissues after scaffold implantation.

Statistical analysis

The first author used the SPSS 11.0 software package to perform the statistical analysis. All data were represented as the mean ± standard

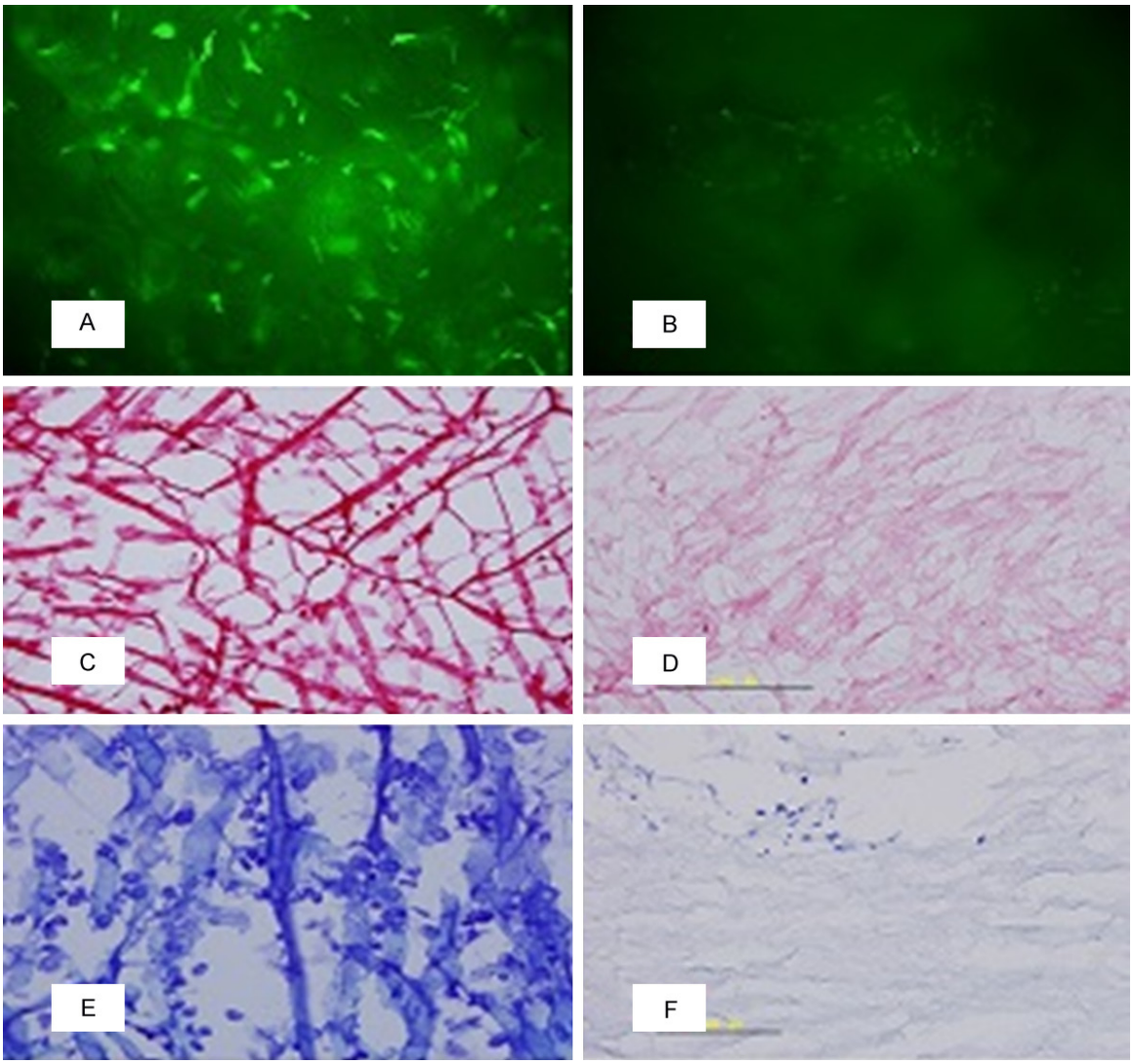

Figure 2. A: The FDA/PI staining showed large numbers of viable cells on the ACECM scaffolds 3 days after seeding. B: The cells at the dense sites of Chondro-Gide were loosely attached. C: Safranin O staining of the ACECM oriented scaffold was positive. D: Safranin O weakly positive in the Chondro-Gide scaffolds. E: The ACECM oriented scaffold was positive for toluidine blue. F: Chondro-Gide scaffold negative for toluidine blue.

deviation, and t-tests were used to make inter-group comparisons. *P*-values less than 0.05 were considered statistically significant.

Results

Physical properties of the scaffolds

The ACECM oriented scaffolds were generally round, white, spongy, and a longitudinal arrangement of the porous channels (**Figure 1A**) was found by SEM. The pore diameter was 150-260 μm, the porosity was 91.75±3.73% (**Figure 1B** and **1C**), and the water absorption expansion coefficient was 35-45%. The Chondro-Gide scaffolds were white, generally square (**Figure 1D**), and the collagen on the superficial layer was dense and transversely arranged with a pore size of 40-100 μm, as found by light microscopy and SEM. Loose, hair-shaped coarse collagen was found in the exterior layer, and the pore size was 50-180 μm, the porosity was 67.75±2.73% (**Figure 1E** and **1F**), and the water absorption expansion coefficient was 10-15%.

Histology

The FDA/PI staining showed large numbers of viable cells on the ACECM scaffolds 3 days

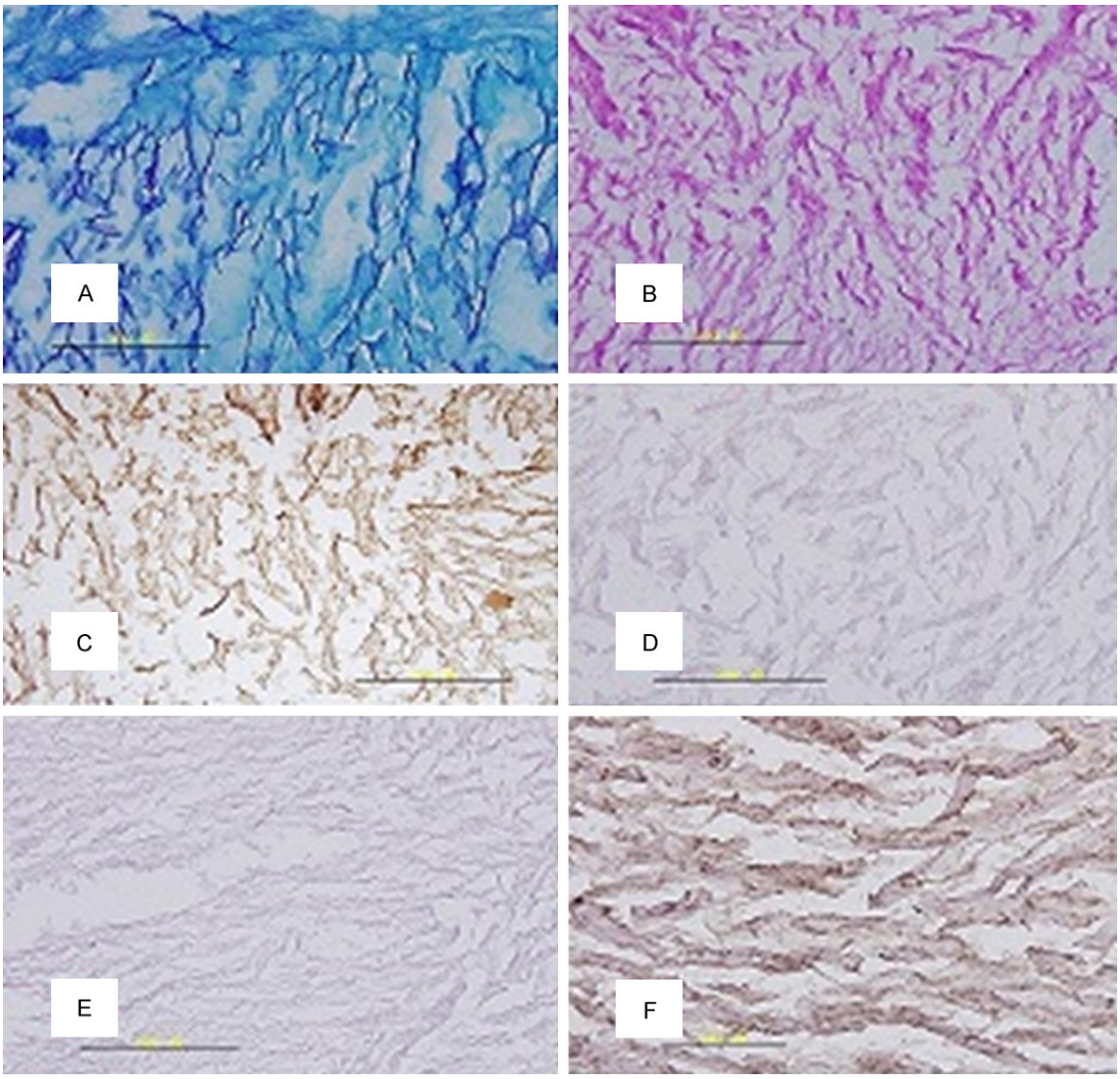

Figure 3. A: The ACECM oriented scaffold was also positive for alcian blue. B: Chondro-Gide scaffold negative for alcian blue. C: The ACECM oriented scaffold was positive for collagen type II. D: The Chondro-Gide scaffold was negative for collagen type II. E: The ACECM oriented scaffold was negative for collagen type I. F: Chondro-Gide scaffold was positive for collagen type I.

after seeding (**Figure 2A**), and a good number of viable cells were also found on the pores of the Chondro-Gide scaffold. The cells at the dense sites were loosely attached (**Figure 2B**). HE staining showed that the ACECM oriented scaffolds were porous and that the collagen filaments were relatively thin. The collagen filaments of the Chondro-Gide scaffolds were thick and randomly oriented. Safranin O staining of the ACECM oriented scaffold was positive, but only weakly positive in the Chondro-Gide scaffolds (**Figure 2C** and **2D**). The ACECM oriented scaffold was positive, and Chondro-Gide scaffold negative, for toluidine blue (**Figure 2E** and **2F**). The ACECM oriented scaffold was also positive, and the Chondro-Gide scaffold negative, for alcian blue (**Figure 3A** and **3B**). The ACECM oriented scaffold was positive for collagen type II, and the Chondro-Gide scaffold was negative (**Figure 3C** and **3D**). Finally, the ACECM oriented scaffold was negative for collagen type I, and the Chondro-Gide scaffold was positive (**Figure 3E** and **3F**).

Mechanical properties

The elastic modulus of the ACECM oriented scaffold was 3.30±0.23 MPa, which was sig-

Table 2. The cytocompatibility of the two scaffolds was assessed using the MTT assay

	Group I	Group II	Group III	Group V
First day	0.287	0.284	0.298	0.308
Third day	0.512	0.492	0.487	0.493
Fifth day	0.798	0.765	0.742	0.774
Seventh day	1.717	1.605	1.677	1.766

Table 3. Comparison of Total collagen, GAG, and DNA content

	Hydroxyproline	GAG	DNA
4131	10.42±2.73	25.12±4.12	10.52±5.79
4132	2.09±1.05	21.74±5.79	7.31±4.37
P value	0.0079	0.4563	0.7427

nificantly higher (P<0.05) than that of the Chondro-Gide scaffold, 1.36±0.20 MPa. The compression stiffness of the ACECM oriented scaffold was 6.67±0.47 N/mm, also significantly higher (P<0.05) than that of the Chondro-Gide scaffold, 2.74±0.41 N/mm.

Cytocompatibility

The cytocompatibility of the two scaffolds was assessed using the MTT assay (**Table 2**). The cytotoxicity of the scaffolds was assessed using the relative growth rate as (PGR) grade 0-1, indicating that both types of scaffolds were less cytotoxic than many cytotoxic materials, based on the cytotoxicity assessment method issued by the CFDA.

Cell adhesion

The adhesion of the seeded cells onto the ACECM oriented scaffold at 3 hours was 68% and at 6 hours was 86%. The adhesion rate of the Chondro-Gide-4132 scaffolds at 3 hours was 52% and at 6 hours was 74%. The cell adhesion onto the ACECM oriented scaffold was faster than that onto the Chondro-Gide scaffold.

Total collagen, GAG, and DNA contents

The hydroxyproline of the ACECM oriented scaffold was 10.42±2.73, which was significantly higher (P<0.05) than that of the Chondro-Gide scaffold, 2.09±1.05. The GAG and DNA of the ACECM oriented scaffold were 25.12±4.12 and 10.52±5.79 respectively, also higher than that of the Chondro-Gide scaffold, 21.74±5.79 and 7.31±4.37 respectively, but they did not reach statistical significance (**Table 3**).

Pathological grading

After 7 days of implantation, the reaction degree of the inflammatory cells was less than or equal to grade 2, and no cyst wall was formed. At 15 and 30 days after implantation, the reaction degree of inflammatory cells was less than or equal to grade 1-2, and no cyst wall was formed. These results put the scaffolds into the category of 'qualified'.

RT-PCR analysis

The Col I gene expression of the ACECM oriented scaffold was 0.41±0.14, which was significantly lower (P<0.01) than that of the Chondro-Gide scaffold, 1.63±0.21; The Col II gene expression of the ACECM oriented scaffold was 4.31±0.54, which was significantly higher (P<0.01) than that of the Chondro-Gide scaffold, 0.24±0.11; The aggrecan gene expression of the ACECM oriented scaffold was 3.76±0.41, which was significantly higher (P<0.01) than that of the Chondro-Gide scaffold, 1.26±0.13; The Sox-9 gene expression of the ACECM oriented scaffold was 0.57±0.08, which was significantly lower (P<0.01) than that of the Chondro-Gide scaffold, 3.07±0.41; The Col X gene expression of the ACECM oriented scaffold was 0.13±0.05, which was significantly lower (P<0.01) than that of the Chondro-Gide scaffold, 7.56±1.21 (**Table 4**; **Figure 4**).

Discussion

Articular cartilage defects are clinically common diseases and can occur for a variety of reasons. Induced arthralgia and functional incapacitation are the most common causes of disability among middle-aged and elderly people [4]. Researchers have been trying to find better approaches to repair articular cartilage defects. Many surgical intervention therapies have been used, such as subchondral bone drilling [5], grinding arthroplasty [6], microfracture [7], autologous cartilage-bone grafting [8], autologous periosteal and cartilage transplantation, and allogenic cartilage transplantation [9]. Among the above methods. Conservative drug therapies have also been tried, but the efficacy is not satisfactory, with most of these treatment modalities yield fibrous repair cartilage [10, 11] for the lack of the durability and mechanical properties of normal hyaline cartilage. Immunologic rejection can occur after

Table 4. RT-PCR analysis of two cartilage tissue engineering materials

	Col I	Col II	Aggrecan	Sox-9	Col X
4131	0.41±0.14	4.31±0.54	3.76±0.41	0.57±0.08	0.13±0.05
4132	1.63±0.21	0.24±0.11	1.26±0.13	3.07±0.41	7.56±1.21
P value	P<0.01	P<0.01	P<0.01	P<0.01	P<0.01

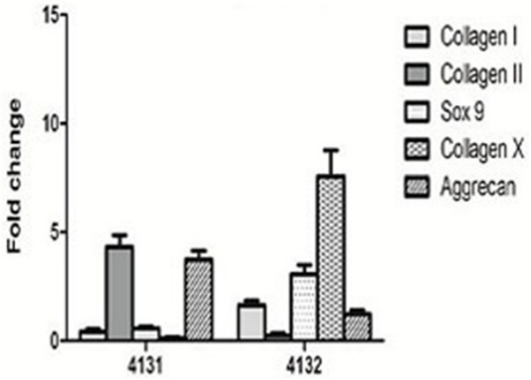

Figure 4. The gene expression of the ACECM oriented scaffold and Chondro-Gide.

allogenic cartilage transplantation. While periosteal transplantation can generate new cartilages in the defect area, endochondral bone formation can also occur at the same time and there is a limited supply of donor tissues, which is a disadvantage of autologous cartilage-bone grafting as well. The donor site morbidity in such cases can be difficult to endure for many patients. Joint replacement with a prosthesis resolve the problems in some patients, but revisions are sometimes necessary and the cost is high. Given the shortcomings of the above therapies, WE are forced to find more effective methods to treat cartilage defects. Tissue engineering strategies make novel and promising treatments to repair injured cartilage.

As we understand the functions, components, and structures of articular cartilage as more as possible, the focus of tissue-engineered cartilage repair has shifted from creating tissue-engineered cartilage that looks histologically like cartilage to creating functional articular cartilage. For example, the wear resistance of repaired tissues can be improved. To achieve this goal, high requirements are needed for the tissue-engineering cartilage constructed in vitro. Because the components and spatial structure of articular cartilage determine its function, assuming that the appropriate cells can be seeded and the basic tissue-engineered scaffold conditions can be satisfied, the chemical composition and spatial configuration of the microenvironment surrounding the cartilage cells must be taken into consideration.

Many studies have reported materials for cartilage tissue engineering [12]. However, most of these materials lack similar structures and components, including collagen type II and proteoglycans that are inherent in articular cartilage-based scaffolds. Therefore, these materials cannot provide sufficient cell density and growth rates [13]. Several studies have reported that cells have the highest proliferation rate when seeded on collagen type II compared to 3 other types of collagen membranes [14]. Similarly, the amount of apoptosis was higher for cells seeded on membranes of collagen type I/III than on those on type II collagen membranes [15].

Chondro-Gide is marketed as a cartilage injury repairing scaffold which has been widely applied as a clinical treatment, and shows good therapeutic efficacy [16-18]. The components of Chondro-Gide are extracted from veterinarian-verified pigs, and mostly include types I and III collagen in the native bimolecular structure of the pigs. The Chondro-Gide scaffolds have a smooth surface and a porous surface. When used, the porous surface is oriented towards the cartilage defect and the smooth surface faces the articular cavity. The porous surface is relatively rough, facilitating the adhesion of cartilage cells, while the smooth surface is relatively dense, preventing postoperative cell leakage. During the surgery, this membrane can be directly attached to the injury region and additional cutting of the periosteum is unnecessary. Therefore, various potential complications arising from the transplantation of periosteum onto the surface of the injured regions can be avoided. However, the components, structures, and biological and mechanical properties of this type of scaffold are significantly different from natural cartilage, and the long-term effects still remained to be further verified.

Because of the similarity between the extracellular matrix of porcine articular cartilage and normal human articular cartilage, the use of

porcine articular cartilage extracellular matrix to prepare oriented scaffolds for articulate cartilage repair has become a popular approach. The main chemical components of articular cartilage extracellular matrix are GAGs and type II collagen, which play an important role in determining the cartilage function and maintaining the phenotype of the cartilage cells. The organic component with the highest content in cartilage matrix is type II collagen, which is the characteristic insoluble collagen protein in hyaline cartilage and closely binds to GAGs. Type II collagen is histocompatible, non-poisonous, non-immunogenic, and compatible with cartilage cells in vitro, maintaining their phenotype and functions. In this study, we compare the effects of the ACECM-derived oriented scaffolds with the Chondro-Gide scaffolds to verify the feasibility and safety of their clinical application.

The adhesion and proliferation of seeded cells, and the biosynthesis and deposition of extracellular matrix, depend on whether the cell scaffold provides sufficient open space and surface area for the seeded cells. The most important parameters of the porous structure of the ACECM oriented scaffolds are the porosity and pore size, which directly affect the interactions between the scaffolds and seeded cells. Several studies have indicated that pores with diameters greater than 100 μm provide a relatively large adhesion area, facilitating cell adhesion by providing nutrients and gas exchange and waste excretion with the surrounding environment. This also further promotes the proliferation and differentiation of the cells. Therefore, the pore diameter and porosity of scaffolds should be among the first properties considered when designing and preparing scaffolds for cartilage tissue engineering. The surface area for cell adhesion is determined by the porosity, as well as the entry and distribution of seeded cells, while the discharge of metabolic products and the supply of nutrition are affected by both pore diameter and porosity. Pore diameters of 100 to 250 μm and porosities greater than 90% have been reported to be the most beneficial for tissue growth [19]. The pore diameter of the ACECM oriented scaffolds prepared here ranged from 150 to 260 μm, and the porosity was 91.75±3.73%. Thus, the scaffolds should provide suitable three-dimensional space for the attachment and proliferation of stem cells and facilitate their differentiation into cartilage.

The hydrophilicity of a scaffold is another important material factor, and improving the hydrophilicity of a material is an important step towards creating better tissue-engineered cartilage constructs. Cells seeded on hydrophobic materials often appear clogged on the scaffold surface because of surface tension, making it difficult for the cells to enter the scaffold. However, hydrophilic scaffold materials facilitate cell entry and adhesion. The ACECM oriented scaffolds were relatively hydrophilic compared to the Chondro-Gide scaffolds, which facilitates the exchange of nutrients and the discharge of metabolic products, prevents the efflux of interstitial fluid and nutritional substances, facilitates cell proliferation and tissue regeneration, and is satisfactory for a cartilage tissue-engineered scaffold.

The ACECM oriented scaffolds mimic the spatial configuration of normal articular cartilage and display higher mechanical properties than those of the Chondro-Gide scaffold. This suggests the potential to use the scaffolds to construct functional cartilage in vivo.

Assessing the cytotoxicity of a scaffold in cell culture has the advantages of being simple, low cost, highly sensitive, and requiring a short test cycle, among others. Therefore, we evaluated the cytotoxicity of the scaffolds to indicate safety according to the biomaterial safety evaluation standards issued by the Ministry of Health, which is an important approach to the evaluation of the histocompatibility of biomaterials. The mode of contact between the cells and the scaffolds is classified as contact with the material leaching liquor or direct contact, and the method used to evaluate the cytotoxicity is the MTT colorimetric assay to determine the cell viability.

Because this method is easy to perform and low-cost, creating no environmental pollution, it is widely used. The basic principle is that exogenous methyl thiazolyl tetrazolium (MTT) salt can be reduced by the succinate dehydrogenase in the mitochondria of living cells to form the insoluble blue crystal formazan, which is then deposited inside the cells. The number of living cells and their functional status are positively correlated with the number of crystals formed, within a certain range, because the assay depends on cell mitochondria, which are the most important cell organ for energy

metabolism, and the number of functioning mitochondria increases during cell proliferation and active metabolism, decreases during decay, and reaches zero after cell death. In cases of abundant cell growth, when the cell morphology is appropriate and the cells are at a high density, a deep color and high OD develops. The determination of OD is made on the dye based on defined numbers of cells as standards, and the relative growth rate of experimental cells can be detected and calculated by comparison with the standards. The relative growth rate of the cells can then be converted into a cytotoxicity level as a quantitative measure. Therefore, the MTT assay is a good method to sensitively indicate the degree of cell lesions [20]. The experiments reported here used L929 cells directly as the detection cells. On the admimistration of the MTT method, the growth and proliferation of this cell was determined in order to evaluate the cytotoxicity of the novel biological cartilage scaffolds. The L929 cells showed a relatively high level of proliferation on both types of scaffolds. The growth and proliferation of the cells increased over time. The calculated proliferation equations for the two groups were similar, and the growth curves basically coincided, indicating that the ACECM oriented scaffold was a suitable carrier for seeded cells.

Many factors after the time require adhesion of cells, including the material physicochemical properties and surface condition, the time of contact between the material and cells, the nature of the cell membrane, and cell metabolism, making cell adhesion an important parameter for assessing the overall biocompatibility of a material. The results of the cell adhesion experiment indicated that cells adhered well to the ACECM scaffold, with 68% adhesion at 3 hours and 86% adhesions at 6 hours. This suggested that the cells seeded on the scaffolds diffused relatively rapidly and were able to homogeneously infiltrate the scaffold interiors. Cell adhesion to the scaffolds was determined by counting the non-adhered cells, and the adhesion increased over time, within a certain period. Many factors are predicted to contribute to cell adhesion, including that the scaffolds which are made from natural biological tissues and retain the original structural environment for cell growth; the main components, type II collagen and GAGs, facilitate cell adhesion; the water absorption expansion coefficient effectively prevents the efflux of interstitial fluid and nutritional substances; the 3D porous structure provides a relatively large surface area for cell adhesion; and the interconnected pore structure facilitates the discharge of metabolic products and nutritional exchange, provides sufficient space for cell attachment, and is conductive to their proliferation, growth, and differentiation.

The total collagen content of the ACECM oriented scaffolds was higher than that of the Chondro-Gide scaffolds, but no significant differences in GAG and DNA were found. This further suggests that the ACECM oriented scaffolds have similar extracellular matrix composition as collagen and have very low immunogenicity. After the scaffolds were subcutaneously implanted in rats, the pathological grading indicated that the pathological rates of the two types of scaffolds are qualified, further demonstrating that both scaffolds have low immunogenicity, minimal toxicity, and are appropriate for clinical application.

Located on the long arm of chromosome 17, the SOX family gene SOX-9 plays important roles in male sexual development, regulating the differentiation and development of cartilage, and as the main transcription factor that regulates chondrogenesis. Type II collagen is an important marker for cartilage cells. Aggrecan is a large proteoglycan molecule that plays an important role in the extracellular matrix of cartilage, is vital for cartilage cell health, and helps maintain a consistent expression of type II collagen in time and space to protect the structure and function of the cartilage tissue. SOX-9 regulates cartilage differentiation mainly by combining type II collagen with the characteristic cartilage cells and aggrecan protein as a gene enhancer to achieve activated expression.

SOX-9 can also protect the cartilage cell phenotypes by binding with and activating the enhancer sequence of non-cartilage cell cartilage genes. In addition, SOX-9 can also induce bone morphogenetic protein expression in cartilage. As shown by the results, cartilage cells have different expression levels of genes after seeding on the two types of scaffolds. The expression of Col II and aggrecan after seeding on the ACECM scaffolds was higher than those of cells seeded

on the Chondro-Gide scaffolds, and the expression of SOX-9 and Col X was lower than those of cells on the Chondro-Gide scaffolds. This suggests that ACECM oriented scaffolds can properly maintain the differentiation state of cartilage cells.

In contrast with the Chondro-Gide scaffolds, the ACECM oriented scaffold is composed of components and oriented structures that resemble normal cartilage. This replication of the microenvironment of the cartilage cells provides several advantages. First, as the template for the regenerative tissues after cell seeding, the scaffolds help guide the seeded cells and the alignment and orientation of the newly secreted extracellular matrix, as well as deciding the shape, structure, and function of the developing tissue. Oriented scaffolds have a vertically oriented porous channel structure, similar to the aligned columnar structure of normal articular cartilage. The internal fibers also present a linear, longitudinal distribution that is beneficial for creating a longitudinal distribution and alignment of seeded cells, similar to the distribution and alignment of the structures of the deep layer of articular cartilage. Second, the elastic modulus of the oriented scaffolds in the direction of orientation and the compression stiffness were found to be higher than those of the Chondro-Gide scaffolds. In fact, the mechanical properties of the ACECM oriented scaffold were similar to those of native articular cartilage, indicating that the oriented alignment of the fibers has a significant effect on the mechanical properties of scaffolds. This mechanical strength is of vital importance during the formation of new tissues, where the maintenance and protection of the seeded cells from injurious stresses before maturation is necessary. Third, because of the connectivity of the internal porous channels, the ACECM oriented scaffolds facilitate the homogeneous distribution of seeded cells into the scaffold interiors, facilitate the entry and exit of nutritional substances, metabolic products, and biomacromolecules, thereby avoiding the "hollow phenomenon" that frequently arises during in vitro culture after scaffolds are seeded with cells [21, 22]. Such types of scaffolds suggest the possibility of achieving functional cartilage repair.

In conclusion, comparisons between a novel ACECM oriented scaffold and the commercially available Chondro-Gide scaffold indicated that the ACECM oriented scaffolds performed better than the Chondro-Gide scaffolds in vitro, indicating the potential benefits of the ACECM cartilage tissue-engineered scaffold.

Acknowledgements

This work was funded by the Beijing Metropolis Beijing Nova Program (2011115), the National Natural Science Foundation of China (General Program) (31170946), the National Natural Science Foundation of China (Youth Program) (31100696), the National Natural Science Foundation of China (81472092), the National High Technology Research and Development Program of China (2012AA020502), the People's Liberation Army 12th Five-Year Plan Period (Key Program) (BWS11J025), the National Basic Research Program of China (973 Program) (2012CB518106), the National Natural Science Foundation of China (Key Program) (21134004), and the New Drug Creation of the Special Ministry of Science and Technology.

Disclosure of conflict of interest

None.

Address correspondence to: Dr. Peilan Wang, Outpatient Department, PLA General Hospital, 28 Fuxing Road, Haidian, Beijing 100853, P. R. China. Tel: 13321166780; 010-66939335; Fax: 13321166780; 010-66939335; E-mail: wangpeilan301@163.com

References

[1] Moreira-Teixeira LS, Georgi N, Leijten J, Wu L, Karperien M. Endocr Dev 2011; 21: 102-115.

[2] Kock L, van Donkelaar CC and Ito K. Tissue engineering of functional articular cartilage: the current status. Cell Tissue Res 2012; 347: 613-27.

[3] Wang ZM and Peng J. Articular Cartilage Tissue Engineering: Development and Future: A Review. Journal of Musculoskeletal Pain 2014; 22: 68-77.

[4] Buckwalter JA and Mankin HJ. Articular cartilage: degeneration and osteoarthritis, repair, regeneration, and transplantation. Instr Course Lect 1998; 47: 487-504.

[5] Insall J. The Pridie debridement operation for osteoarthritis of the knee. Clin Orthop Relat Res 1974; 61-7.

[6] Minas T and Nehrer S. Current concepts in the treatment of articular cartilage defects. Orthopedics 1997; 20: 525-538.
[7] Steadman JR, Rodkey WG and Rodrigo JJ. Microfracture: Surgical technique and rehabilitation to treat chondral defects. Clin Orthop Relat Res 2001; S362-S369.
[8] Outerbridge HK, Outerbridge AR and Outerbridge RE. The use of a lateral patellar autologous graft for the repair of a large osteochondral defect in the knee. J Bone Joint Surg Am 1995; 77: 65-72.
[9] Kwan MK, Wayne JS, Woo SL, Field FP, Hoover J, Meyers M. Histological and biomechanical assessment of articular cartilage from stored osteochondral shell allografts. J Orthop Res 1989; 7: 637-44.
[10] Messner K and Gillquist J. Cartilage repair. A critical review. Acta Orthop Scand 1996; 67: 523-9.
[11] Richardson JB, Caterson B, Evans EH, Ashton BA and Roberts S. Repair of human articular cartilage after implantation of autologous chondrocytes. J Bone Joint Surg Br 1999; 81: 1064-8.
[12] Iwasa J, Engebretsen L, Shima Y and Ochi M. Clinical application of scaffolds for cartilage tissue engineering. Knee Surg Sports Traumatol Arthrosc 2009; 17: 561-77.
[13] Gavénis K, Schmidt-Rohlfing B, Mueller-Rath R, Andereya S and Schneider U. In vitro comparison of six different matrix systems for the cultivation of human chondrocytes. In Vitro Cell Dev Biol Anim 2006; 42: 159-67.
[14] Gigante A, Bevilacqua C, Cappella M, Manzotti S and Greco F. Engineered articular cartilage: influence of the scaffold on cell phenotype and proliferation. J Mater Sci Mater Med 2003; 14: 713-6.
[15] Gille J, Meisner U, Ehlers EM, Müller A, Russlies M and Behrens P. Migration pattern, morphology and viability of cells suspended in or sealed with fibrin glue: A histomorphologic study. Tissue Cell 2005; 37: 339-348.
[16] Kon E, Filardo G, Condello V, Collarile M, Di Martino A, Zorzi C and Marcacci M. Second-generation autologous chondrocyte implantation results in patients older than 40 years. Am J Sports Med 2011; 39: 1668-1675.
[17] Berninger MT, Wexel G, Rummeny EJ, Imhoff AB, Anton M, Henning TD and Vogt S. Matrix-assisted autologous chondrocyte transplantation for remodeling and repair of chondral defects in a rabbit model. J Vis Exp 2013; e4422.
[18] Gille J, Behrens P, Volpi P, de Girolamo L, Reiss E, Zoch W and Anders S. Outcome of Autologous Matrix Induced Chondrogenesis (AMIC) in cartilage knee surgery: data of the AMIC Registry. Arch Orthop Trauma Surg 2013; 133: 87-93.
[19] Whang K, *et al.* A Novel Method to Fabricate Bioabsorbable Scaffolds. Polymer 1995; 36: 837-842.
[20] Lee SH, *et al.* An Image Cytometric MTT Assay as an Alternative Assessment Method of Nanoparticle Cytotoxicity. Bulletin of the Korean Chemical Society 2014; 35: 1933-1938.
[21] Freed LE, Martin I and Vunjak-Novakovic G. Frontiers in tissue engineering. In vitro modulation of chondrogenesis. Clin Orthop Relat Res 1999; Suppl: S46-58.
[22] Silva MM, Cyster LA, Barry JJ, Yang XB, Oreffo RO, Grant DM, Scotchford CA, Howdle SM, Shakesheff KM, Rose FR. The effect of anisotropic architecture on cell and tissue infiltration into tissue engineering scaffolds. Biomaterials 2006; 27: 5909-17.